

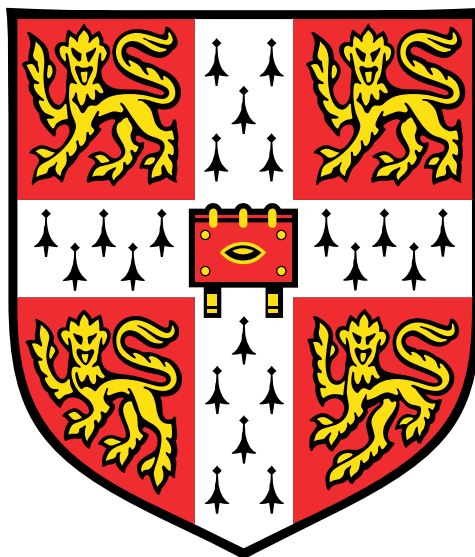
Mechanics of Human Bone

Lateral Hinge Fracture in High Tibial Osteotomy

Stanisław Tomaszczyk

King's College

The project submitted for the degree of
Master of Engineering



Engineering Department
University of Cambridge
United Kingdom

26-05-2020

Technical Abstract

Medial opening wedge high tibial osteotomy (MOWHTO for short) is a surgery aimed at correcting the varus deformity of the knee - one of the primary causes of knee osteoarthritis. It achieves this by adjusting the geometry of the proximal tibia. A cut is made through the bone using a surgical saw, it is then opened up by a desired angle and finally fixed in place using screws and a support plate. The bone then takes a couple of weeks to grow and fill the wedge, after which the support plate is removed. The surgery is known to be very effective at reducing the loads acting on the medial compartment of the knee joint and therefore hindering the progression of osteoarthritis but it is also associated with multiple complications. The most common of them is the lateral hinge fracture.

The osteotomy cut does not penetrate all the way through the bone in this surgery and the lateral hinge is the portion of the tibia that is left in front of it. When the wedge is opened up a stress concentration arises within the bone cortex at the apex of the osteotomy cut and eventually causes a crack to nucleate. The Takeuchi fracture classification is commonly used to distinguish between the failure modes. Takeuchi type I is the least dangerous type and is associated with the crack propagating horizontally through the lateral cortex. Types II and III are more dangerous and have the fracture propagate vertically downwards below the tibiofibular joint and upwards to the tibial plateau respectively.

An investigation into the surgical guidelines for MOWHTO shows that the position of the apex of the cut is very poorly defined. The guidance for lateral hinge width ranges from 5 mm to 15 mm and the distance from the apex to the tibial plateau is defined relative to the tibiofibular joint the position and size of which are highly variable. It is clear that the position of the apex has a very big impact on the mechanics of the surgical process and therefore improving its positioning has a great potential for reducing the incidence of fracture. The aim of this project was therefore to investigate the impact changing the position of the apex has on the fracture risk.

A decision was made to use both experimentation and finite element modelling as two complementary approaches with experiments showing the fracture modes and finite element models outputting the corresponding stress field. The desire to accurately capture the geometry of the proximal tibia led to the use of artificial bones for experimentation and tomography-based 3D finite element models with non-homogeneous mechanical properties for the simulations. However, the limited access to artificial bones as well limited available computational power meant that an alternative approach was needed to be able to draw definitive conclusions. For this reason two separate approaches were developed that in a simplified way captured the two osteotomy apex position regimes. The wide hinge approach dealt with the cases when the apex was far away from the lateral cortex and assumed that the bone geometry around the apex was flat. A finite element model as well as a set of experiments on Perspex samples was performed as a part of this approach. The narrow hinge approach only consisted of a finite element model which captured the stress fields around narrow hinges. It was a 3D model, but because of the local character of the stress field it could be far smaller and hence better performing than the full geometrically accurate one.

In both the artificial bone and the perspex plate experiments the impact of the osteotomy apex position on wedge opening angle at failure, failure load and fracture type were recorded in an opening-to-failure test in an Instron machine. The geometrically accurate finite element model, due to its poor mesh density, was only used for the qualitative assessment of the stress field and as a basis for the further two models. Both in the case of the wide and the narrow hinge model the maximum in-plane principal stress was measured which corresponded to the mode I crack opening stress in the cortex at the apex surface. Additionally, in the wide hinge model

the position of the extreme stress on the apex was measured in order to be able to correlate the stress field with the fracture nucleation location observed in the experiments.

Both experiments showed a clear decrease in the wedge opening angle at failure and increase in the failure load as the width of the lateral hinge got larger. Additionally, it was found that type I fractures are recorded for narrower hinges while type III for wider ones. It was noted that all type I fractures nucleated at the upper corner of the rectangular apex profile while type III fractures nucleated at the lower corner. The lateral hinge width at which the fracture type transitions from I to III was found to strongly depend on the apex to joint line distance - it decreased rapidly as the apex moved upwards. Moving it upwards also resulted in a slightly increased opening at failure for all hinge widths.

Both the wide hinge and the narrow hinge simulations showed a clear increase in the extreme crack opening stress as the width of the lateral hinge increased. The wide hinge model also demonstrated how the location of the extreme stress around the apex changed with the apex position and a clear link with the fracture nucleation locations recorded in the experiments was found. The stress results from the two models were combined to obtain the relationship across the whole regime and the outcome was used in a probabilistic analysis. The assumption that the true stress is normally distributed around the obtained value of mean stress was used to convert the relationship to a failure probability relationship.

The main conclusion of this investigation was that, for a fixed applied displacement (i.e. fixed wedge opening), reducing the hinge width reduces the intra-operative fracture risk. However, robustness of the construct and faster healing process are factors that encourage wider hinges and they would have to be quantified in order to investigate the trade-off and find the optimum hinge width. Similarly, a risk analysis could be performed on the vertical position of the apex to understand the trade-off between the reducing the risk of the more dangerous type III fracture and reducing the overall fracture incidence. The observed correlation between the fracture nucleation location and Takeuchi fracture type is a very useful result in that it allows to predict the failure mode without modelling the fracture event itself. Therefore, this study not only provides useful insight into the impact of the position of the osteotomy apex on the fracture risk in medial opening wedge high tibial osteotomy but also provides a strong basis for future work.

Contents

List of Figures	5
List of Tables	6
1 Introduction	7
2 Background	8
2.1 Clinical Background	8
2.1.1 MOWHTO - Rationale	8
2.1.2 MOWHTO - Procedure and Surgical Details	9
2.1.3 Bone Fracture as a Complication of MOWHTO	11
2.2 Fracture Risk Reduction Strategies - Current State of the Art	13
2.2.1 Proposed Fracture Risk Reduction Strategies	13
2.2.2 Effect of Osteotomy Apex Position	13
2.3 Mechanical Characteristics of Proximal Tibia	14
2.3.1 Bone Structure	14
2.3.2 Mechanical Properties	15
2.4 Finite Element Models	17
3 Aim	17
4 Project Structure	17
5 Experiments	21
5.1 Methods	21
5.1.1 Artificial Bone Experiments	21
5.1.2 Perspex Plate Experiments	24
5.2 Results	25
5.2.1 Artificial Bone Experiments	25
5.2.2 Perspex Plate Experiments	27
6 Finite Element Models	29
6.1 Methods	29
6.1.1 Geometrically Accurate Model	29
6.1.2 Wide Hinge Model	30
6.1.3 Narrow Hinge model	32
6.2 Results	33
6.2.1 Geometrically Accurate Model	33
6.2.2 Wide Hinge Model	34
6.2.3 Narrow Hinge Model	35
7 Discussion	36
7.1 Geometrically Accurate Approach	36
7.2 Wide Hinge Approach	36
7.3 Narrow Hinge Approach	37
7.4 Combined Narrow and Wide Hinge Results	38
7.4.1 Apex Position and Stress	38
7.4.2 Apex Position and Fracture Type	40
7.4.3 Apex Position and Failure Load	40
7.5 Probabilistic Analysis	40
7.5.1 Method	40

7.5.2	Application	42
7.6	Practical Considerations	43
7.7	Limitations and Future Work	43
8	Conclusions	44
9	References	45
A	Appendix - Risk Assessment Retrospective	48
B	Appendix - COVID-19 Disruption	48

List of Figures

1	The three fundamental steps of medial opening wedge high tibial osteotomy: performing the osteotomy cut, wedge opening and fixing the support plate [1].	7
2	The relevant nomenclature associated with the knee joint and the proximal tibia region (based on [2]).	8
3	A summary of geometric guidelines for a planar osteotomy cut in MOWHTO (based on [2]).	11
4	A diagrammatic representation of the Takeuchi fracture classification (based on [3]).	12
5	An enlarged photograph of cancellous bone in bovine femur [4].	14
6	A section through a 3D model of the proximal tibia cortex.	15
7	A schematic representation of the overall approach to modelling and experimentation.	18
8	The top view of a horizontal planar section through the apex of the osteotomy cut and its dependence on the lateral hinge width.	20
9	A comparison of the true and double flat plate geometry of the proximal tibia for a 10 mm lateral hinge width.	21
10	The internal structure of an artificial bone.	22
11	A complete osteotomy performed on an artificial bone.	22
12	A complete set of artificial bone samples.	23
13	The last frame before the fracture event in an artificial bone osteotomy test recording.	23
14	A collection of Perspex samples ready for testing. Each sample is 80 mm wide at the widest point.	24
15	A Perspex sample during a test. The sample is 80 mm wide at the widest point.	25
16	The experimental relationship between the lateral hinge width and the wedge opening at failure obtained using the artificial bones.	25
17	The experimental relationship between the lateral hinge width and the failure load obtained using the artificial bones.	26
18	A visual representation of the observed fracture nucleation patterns relative to the osteotomy apex geometry.	27
19	The experimental relationship between the lateral hinge width and wedge opening at failure for different osteotomy apex heights obtained using the Perspex samples.	27
20	The experimental relationship between the lateral hinge width and the failure load for different osteotomy apex heights obtained using the Perspex samples.	28
21	A 3D bone model used as a basis for the geometrically accurate simulations. . . .	30
22	The 2D proximal tibia model geometry with partitions (a) and resulting mesh density around the apex (b).	31
23	Definition of the maximum stress location measurement.	31
24	Visual representation of the geometric approximations made in designing the narrow hinge model.	32
25	A complete narrow hinge model geometry for a 10 mm wide lateral hinge.	33
26	A comparison between the stress distributions for a 5 mm and a 15 mm lateral hinge at a 10° wedge opening.	33
27	The relationship between the lateral hinge width and the maximum crack opening stress obtained using the wide hinge finite element model.	34
28	The relationship between the lateral hinge width and the maximum crack opening stress obtained using the narrow hinge finite element model.	35
29	A comparison between the finite element meshes around the apex of the osteotomy cut for the geometrically accurate model and the wide hinge model.	36
30	A comparison between the finite element meshes around the apex of the osteotomy cut for the geometrically accurate model and the narrow hinge model.	38

31	A comparison between the stress fields in the narrow hinge model for a 6 mm wide and an 8 mm wide lateral hinge. The contour definitions are the same.	38
32	The relationship between the lateral hinge width and the maximum crack opening stress obtained using both the narrow hinge and the wide hinge finite element models.	39
33	The relationship between the lateral hinge width and the maximum crack opening stress for chosen data-points.	39
34	A proposed procedure for converting FEM and experimental data into a failure probability relationship.	41
35	The relationship between the lateral hinge width and the fracture probability for the apex 16 mm from the joint line.	42

List of Tables

1	A table presenting the advantages and disadvantages of the individual finite element models and experiments.	19
2	A map representing the relationship between the recorded Takeuchi fracture types and the position of the apex of the osteotomy cut in the artificial bone experiments. I stands for Takeuchi type I and III stands for Takeuchi type III.	26
3	A map representing the relationship between the recorded Takeuchi fracture types and the position of the apex of the osteotomy cut for the Perspex experiments. I stands for Takeuchi type I and III stands for Takeuchi type III.	28
4	A map representing the relationship between the relative position of the maximum crack opening stress and the position type of the apex of the osteotomy cut (A, B or C).	35